ChemComm

Accepted Manuscript

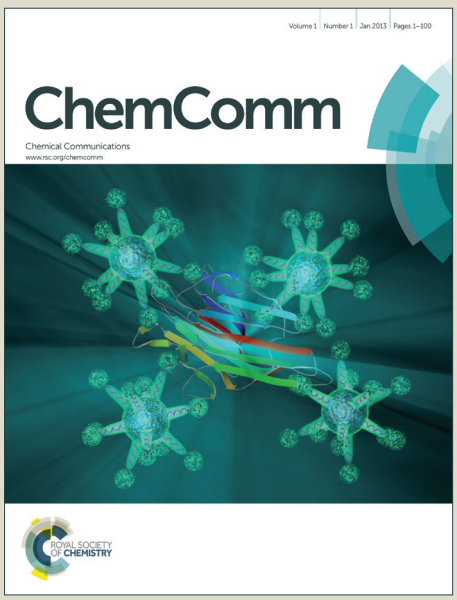

ROYAL SOCIETY OF CHEMISTRY

www.rsc.org/chemcomm

Cite this: DOI: 10.1039/c0xx00000x

www.rsc.org/xxxxxx

ARTICLE TYPE

Understanding $Na_2Ti_3O_7$ as an ultra-low voltage anode material for Na-ion battery

Jing Xu,[a] Chuze Ma,[a] Mahalingam Balasubramanian,[b] Ying Shirley Meng*[a]

Received (in XXX, XXX) Xth XXXXXXXXX 20XX, Accepted Xth XXXXXXXXX 20XX

DOI: 10.1039/b000000x

An in-depth understanding of $Na_2Ti_3O_7$ as Na-ion battery anode is reported. The battery performance is enhanced with carbon coating, due to increased electronic conductivity and reduced solid electrolyte interphase formation. Ti^{4+} reduction upon discharge is demonstrated by in-situ XAS. The self-relaxation behaviour of fully intercalated phase is revealed.

Na-ion batteries have recently gained increased recognition as intriguing candidates for next-generation large scale energy storage systems, stemming from the natural abundance and broad distribution of Na resources. Although the energy density of Na-ion battery is not as high as that of Li-ion battery, which is one of the most dominating energy technologies in this decade, Na-ion batteries operating at room temperature could be suitable for applications where specific volumetric and gravimetric energy density requirements are not as stringent as in EVs, namely in electrical grid storage of intermittent energy produced via renewable sources.[1] This would also contribute to a significant reduction in the costs connected to the use of renewable sources, making Na-ion technology complementary to Li-ion batteries for stationary storage.[2, 3]

For the past several years, it has been realized that because Na ion has a larger ionic radius than Li ion, materials with an open framework are preferred for facile Na ion insertion / extraction. Following this strategy, many breakthroughs in cathode materials have been achieved, such as layered and polyanion compounds.[4] However, the development of suitable anode materials for Na-ion batteries remains a considerable challenge.[5] Graphite cannot be used as anode, since it is unable to accommodate Na ion reversibly.[6, 7] Hard carbons is shown to insert and de-insert Na ions, but the reversibility still requires further improvement.[7, 8, 9] Na-alloys are proposed as possible alternatives, as they can potentially provide higher specific capacities.[10] These alloys, however, suffer from large volume changes upon uptake / removal of Na, in analogy to Li-alloys.[3] Another emerging class of materials is transition metal oxides. For example, $NaVO_2$ is shown to yield a reversible capacity, but its operating voltage is at 1.5 V *vs.* Na^+/Na, leading to a low energy density.[11] Ti-based oxides are suggested to be an attractive alternative, considering that $Li_4Ti_5O_{12}$ is one of the few commercialized anode materials in Li-ion battery.[12] Several different sodium titanates have been explored as anodes for Na-ion battery.[13-15] Among them, a study by Palacín et. al. demonstrated that the layered oxide $Na_2Ti_3O_7$ could reversibly exchange Na ions with the lowest voltage ever

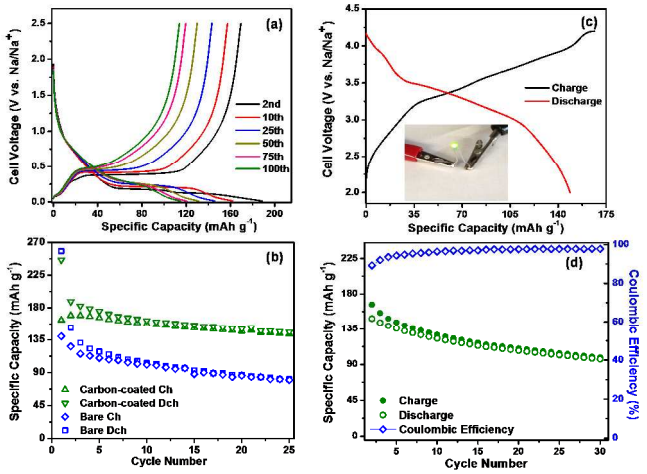

Fig. 1 (a) Voltage profiles of carbon-coated $Na_2Ti_3O_7$ in the 2nd, 10th, 25th, 50th, 75th and 100th cycles at C/10 rate. (b) Cycling performance for carbon-coated and bare $Na_2Ti_3O_7$. (c) Voltage profiles and (d) Cycling performance for the Na full cell.

reported for an oxide insertion electrode.[14] The ultra low voltage and intrinsic high reversibility of this material make it a strong anode candidate for Na-ion battery. Very recently, the same group identified the fully intercalated phase, $Na_4Ti_3O_7$, and provided additional insight on the low intercalation potential, using DFT calculations.[15] However, more work is still required to closely connect the fundamental properties with the battery performance and to systematically evaluate whether it can be a viable anode for Na-ion battery. Herein, we report a comprehensive study to unveil the underlying relationship between its intercalation mechanism and battery performance for $Na_2Ti_3O_7$ anode.

$Na_2Ti_3O_7$ was prepared by a mechanical mixing of anatase TiO_2 and anhydrous Na_2CO_3, followed by calcination at 800 ℃ (for experimental details, see ESI). The as-synthesized material was well crystallized into P21/m space and adopted a pellet shape (Fig. S1). The white color of the obtained powder suggested its intrinsic insulating property, which is undesired for battery application. So carbon coating by sucrose pyrolysis was applied to improve electronic conductivity.[16] The thermogravimetric analysis suggests that the coated material contains 9% carbon. (Fig. S2) The electrochemical properties were tested in Na half cell over a voltage window of 0.01–2.5 V. Fig. S3 presents the first cycle electrochemical profile. The average intercalation

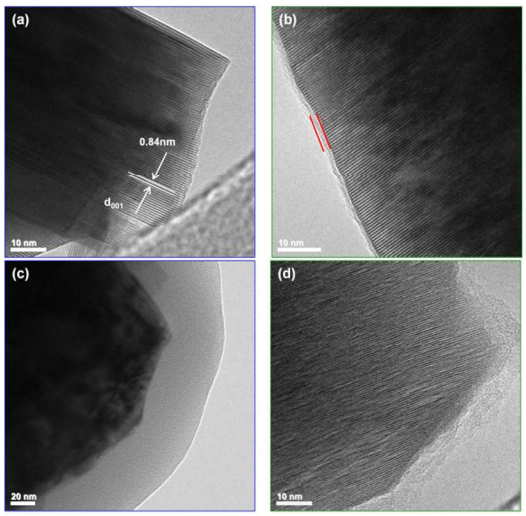

Fig. 2 TEM images for (a) bare and (b) carbon-coated $Na_2Ti_3O_7$ at pristine state. TEM images for (c) bare and (d) carbon-coated $Na_2Ti_3O_7$ after 1st discharge.

potential is around 0.35 V, and a large amount of excess capacity in the first discharge is observed mainly due to irreversible Na intercalation into carbon additive (Super P) in the electrode, consistent with previous literature.[14] Starting from the first charge, the theoretical capacity of 177 mAh g^{-1} (corresponding to 2 Na insertion per formula unit) is fully delivered and more than 115 mAh g^{-1} capacity is well maintained after 100 cycles for the carbon-coated $Na_2Ti_3O_7$ (Fig. 1a). Besides the excellent cycling properties, good rate performance is achieved due to improved electronic conductivity (Fig. S4). Compared with carbon-coated $Na_2Ti_3O_7$, the as-synthesized (henceforth referred to as "bare $Na_2Ti_3O_7$") displays notably reduced capacity (Fig. 1b). Therefore, the coated carbon plays an important role in enhancing the battery performance.

To evaluate the practical application of $Na_2Ti_3O_7$, herein we demonstrate for the first time a full Na cell using $Na_2Ti_3O_7$ as anode material. Fig. 1c is the voltage profile of the $Na_2Ti_3O_7$ / $Na_{0.80}Li_{0.12}Ni_{0.22}Mn_{0.66}O_2$ full cell, in which the cathode material, P2 - $Na_{0.80}Li_{0.12}Ni_{0.22}Mn_{0.66}O_2$, has been reported by us previously.[17] Due to the ultralow voltage of $Na_2Ti_3O_7$ anode, the average voltage of this full cell is as high as 3.1 V, which is comparable to commercial Li-ion battery. As seen in Fig. 1c inset, the Na full cell can easily light up a 2.5 V LED bulb. The cycling of the full cell at C/10 rate is displayed in Fig. 1d. The capacity is stabilized at 105 mAh g^{-1} after 25 cycles (capacity is determined by anode active material). At the same time, the coulombic efficiency is gradually increased to above 98% and maintained in the subsequent cycles. The overall energy density is 100 Wh kg^{-1}, based on the total weight of active materials from both cathode and anode. Although the energy density is lower than that of Li-ion battery, it should be noted that Na does not alloy with Al, so that the Al current collector can be used for both cathode and anode. This will help to further improve energy density of Na-ion battery and reduce manufacturing cost.

High resolution transmission electron microscopy (HRTEM) images revealed the surface morphologies for bare and carbon-coated $Na_2Ti_3O_7$ samples. At pristine state (Fig. 2a and 2b), the lattice fringes are clearly observed, implying good crystallinity. The width (0.84 nm) of neighbouring fringe distance is

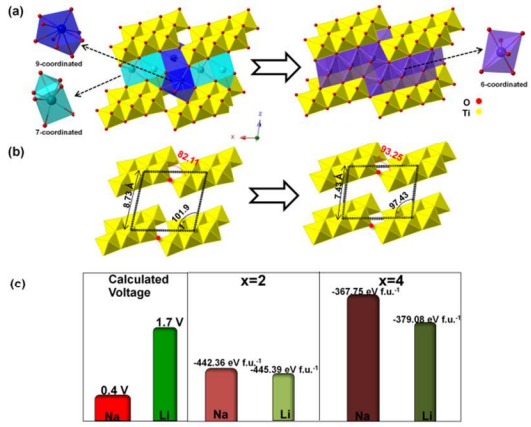

Fig. 3 (a) The phase transformation (b) related structural change upon Na intercalation. (c) The calculated voltage and electrostatic energy at x=2 and x=4 for $Li_xTi_3O_7$ and $Na_xTi_3O_7$ respectively.

corresponded to (0 0 1) plane. As suggested by Fig. 2b, the carbon is uniformly coated on the surface of $Na_2Ti_3O_7$ with a thickness around 3 nm. After 1st discharge, an amorphous layer with a thickness of 30-50 nm is seen on the bare $Na_2Ti_3O_7$ particle (Fig. 2c), indicating a severe side reaction at the solid electrolyte interface (SEI). In contrast, the SEI layer is largely inhibited in the carbon-coated $Na_2Ti_3O_7$ (Fig. 2d). Consequently, it is noticed that the initial coulombic efficiency is increased by 11 % from bare to carbon-coated sample (Fig. S3). This demonstrates that in addition to improving the electronic conductivity, the coated carbon on the surface could also serve as a protection layer to prohibit side reactions of the electrolyte and enhance battery performance. It should be noted that the carbon coating could only partially improve the inefficiency in the 1st cycle, since the main irreversible capacity is resulted from Na react with super P.[14]

In order to understand the structural evolution and the ultra low voltage for $Na_2Ti_3O_7$ upon cycling, the $Na_xTi_3O_7$ as well as its Li analogue $Li_xTi_3O_7$ ($2 \le x \le 4$) was investigated by first principles calculation. The fully intercalated phase, $Na_4Ti_3O_7$, is identified by our calculation, which is in agreement with Dr. Palacin et.al.'s recent report.[15] More details of the phase transformation can be revealed by closely examining structural difference between $Na_2Ti_3O_7$ and $Na_4Ti_3O_7$. As shown in Fig. 3a, although there is no bond broken in Ti-O frameworks, the Na sites experience drastic variations. The Na-ion coordination decreases from 9 and 7 at pristine state to 6 after fully intercalation. In addition, to accommodate more Na ions in the structure, the lattice parameters are adjusted by shearing the Ti-O slabs. The c lattice parameter is reduced due to better screening effect from high Na-ion concentration in Na layer. More interestingly, the dramatic Na site change is not just due to the shift of the Ti-O slab but also from contributions involving modifications within the Ti-O framework. After full intercalation, the joint angle between neighbouring Ti-O blocks is enlarged from 82.11°to 93.25° (Fig. 3b). Therefore, it is fascinating to notice that this type of framework possesses structural flexibility to some degree, which is quite unique compared with traditional layered intercalation compounds, such as $LiCoO_2$. As for the intercalation voltage, the calculated values for both $Na_xTi_3O_7$ and $Li_xTi_3O_7$ are basically consistent with experimental results.[15] (Fig. 3c) Based on Nernst equation, the battery voltage is directly

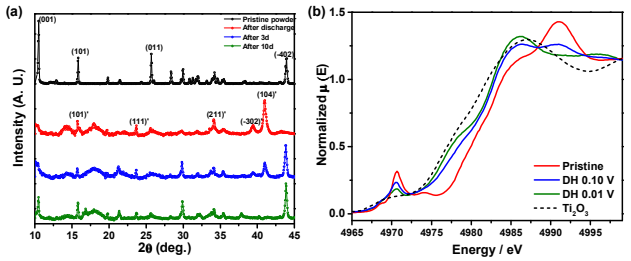

Fig. 4 (a) Change in the XRD patterns with time for fully discharged electrodes. (b) Normalized Ti K-edge XANES for $Na_2Ti_3O_7$ at pristine state (red), after discharged to 0.10 V (blue), and after discharged to 0.01 V (green).

related to the Gibbs free energy change during chemical reaction. Thus, the lower voltage for $Na_xTi_3O_7$ compared with $Li_xTi_3O_7$ is associated with the smaller change in Gibbs free energy in the Na case. In addition, we have studied the electrostatic interaction in the crystal structure using Ewald summation.[18] It is interesting to see that there is a bigger jump in electrostatic energy for $Na_xTi_3O_7$ from x=2 to x=4 than that for $Li_xTi_3O_7$, demonstrating a much stronger electrostatic repulsion in $Na_4Ti_3O_7$. Such large electrostatic repulsion leads to structural instability and consequently, increases the Gibbs free energy for $Na_4Ti_3O_7$. Therefore, the overall change in Gibbs free energy upon intercalation is reduced in Na case and the voltage is lowered accordingly.

Owing to the strong electrostatic repulsion in the fully discharged phase, $Na_4Ti_3O_7$, a "self-relaxation" behaviour was observed. As shown in Fig. 4a, the diffraction pattern for $Na_4Ti_3O_7$ phase is obtained right after the full discharge was completed. However, for the electrodes stored in the glovebox for 3 and 10 days after full discharge, the intensity of peaks from $Na_4Ti_3O_7$ phase, such as (-3 0 2) and (1 0 4), gradually and systematically diminishes. Concomitantly, the diffraction peaks from the $Na_2Ti_3O_7$ phase increases steadily. These observations suggest that the $Na_4Ti_3O_7$ structure undergoes self-relaxation. This property is also captured electrochemically. Fig. S5a and S5b compare the voltage profiles for $Na_2Ti_3O_7$ under cycling with and without interval rest (between charge and discharge) respectively. It is observed that the open circuit voltage for the cell with interval rest is increased gradually during the rest time, indicating the structural relaxation. Additionally, though the discharge performances are identical in the two cases, the cell with interval rest can only deliver 130 mAh g^{-1} capacity in the first charge and further decay is seen in the subsequent cycles (Fig. S5c and Fig. S6). Considering that this self-relaxation in the anode material would lead to self-discharge in the actual full cell, it could be one of the main bottlenecks using $Na_2Ti_3O_7$ as anode for Na-ion battery in practice.

The electronic transition was detected by in-situ X-ray absorption spectroscopy (XAS). Customized coin cells were used to prevent the sample contamination. As Ti^{3+} is extremely sensitive to oxidization (Ti^{3+}->Ti^{4+}), any ex-situ characterization attempts to detect Ti reduction during lithiation process were not successful. It is important to make sure that throughout the entire characterization process, the electrodes were never exposed to the ambient environment. In Fig. 4b, the Ti-K edge is gradually shifted towards lower energy region from pristine state to 0.01 V. The shape and position of the pre-edge as well as the position of the main edge for the fully discharged sample approach those found for Ti_2O_3, demonstrating that Ti^{4+} is reduced upon Na-ion intercalation. The decrease in the pre-edge peak is ascribed to the reduced hybridization between Ti-3d and O-2p orbitals during Ti ion reduction.[19, 20] In fact, this Ti reduction is similar to its Li counterparts.[19, 21] Therefore, it is speculated that the ultra-low voltage for $Na_2Ti_3O_7$ material during intercalation could mainly originate from crystal structural perspective as discussed above, instead of electronic contribution.

In summary, a comprehensive study on $Na_2Ti_3O_7$ as an ultra-low voltage anode for Na-ion batteries is reported. The cyclability and coulombic efficiency are significantly enhanced, due to increased electronic conductivity and reduced SEI formation by carbon coating. Na full cell with high operating voltage is demonstrated by taking advantage of the ultra-low voltage of $Na_2Ti_3O_7$ anode. The self-relaxation behaviour for fully intercalated phase, $Na_4Ti_3O_7$, is shown for the first time, which results from structural instability as suggested by first principles calculation. Ti^{4+} / Ti^{3+} is the active redox couple upon cycling based on XANES characterization. These findings unravel the underlying relation between unique properties and battery performance of $Na_2Ti_3O_7$ anode, which should ultimately shed light on possible strategies for future improvement.

Jing Xu and Chuze Ma equally contributed to this work. The authors are grateful for the financial support from the National Science Foundation under CAREER Award Number 1057170. The XAS work was performed at 20-BM-B at Argonne's Advanced Photon Source (APS); the APS is supported by the USDOE under contract No. DE-AC02-06CH11357. The authors appreciate the fruitful discussion and assistance from Dr. Dae Hoe Lee and Mr. James Somerville at the University of California San Diego.

Notes and references

[a] *Department of NanoEngineering, University of California San Diego, 9500 Gilman Drive, La Jolla, CA 92093, USA. E-mail: shirleymeng@ucsd.edu*

[b], *X-ray Science Division, Advanced Photon Source, Argonne National Laboratory, 9700 South Cass Avenue, Argonne, Illinois 60439, USA*

† Electronic Supplementary Information (ESI) available: [details of any supplementary information available should be included here]. See DOI: 10.1039/b000000x/

1 B. L. Ellis and L. F. Nazar, *Current Opinion in Solid State & Materials Science*, 2012, **16**, 168.

2 H. L. Pan, Y. S. Hu and L. Q. Chen, *Energy & Environmental Science*, 2013, **6**, 2338; V. Palomares, M. Casas-Cabanas, E. Castillo-Martinez, M. H. Han and T. Rojo, *Energy & Environmental Science*, 2013, **6**, 2312.

3 M. Valvo, F. Lindgren, U. Lafont, F. Bjorefors and K. Edstrom, *Journal of Power Sources*, 2014, **245**, 967.

4 J. Xu, D. H. Lee and Y. S. Meng, *Functional Materials Letters*, 2013, **6**; M. R. Palacin, *Chemical Society Reviews*, 2009, **38**, 2565.

5 K. Sung-Wook, S. Dong-Hwa, M. Xiaohua, G. Ceder and K. Kisuk, *Advanced Energy Materials*, 2012, **2**, 710; M. D. Slater, D. Kim, E. Lee and C. S. Johnson, *Advanced Functional Materials*, 2012.

6 G. E. Pascal and M. Fouletier, *Solid State Ionics*, 1988, **28**, 1172.

7 D. A. Stevens and J. R. Dahn, *Journal of the Electrochemical Society*, 2001, **148**, A803.

8 *Journal of the Electrochemical Society*, 2000, **147**, 1271; *Journal of the Electrochemical Society*, 2000, **147**, 4428.

9 R. Alcantara, J. M. Jimenez-Mateos, P. Lavela and J. L. Tirado, *Electrochemistry Communications*, 2001, **3**, 639; S. Komaba, W. Murata, T. Ishikawa, N. Yabuuchi, T. Ozeki, T. Nakayama, A. Ogata,

K. Gotoh and K. Fujiwara, *Advanced Functional Materials*, 2011, **21**, 3859.

10 A. Darwiche, C. Marino, M. T. Sougrati, B. Fraisse, L. Stievano and L. Monconduit, *Journal of the American Chemical Society*, 2012, **134**, 20805; X. Yunhua, Z. Yujie, L. Yihang and W. Chunsheng, *Advanced Energy Materials*, 2013, **3**, 128; L. Wu, P. Pei, R. J. Mao, F. Y. Wu, Y. Wu, J. F. Qian, Y. L. Cao, X. P. Ai and H. X. Yang, *Electrochimica Acta*, 2013, **87**, 41; M. Shimizu, H. Usui and H. Sakaguchi, *Journal of Power Sources*, 2014, **248**, 378.

11 C. Didier, M. Guignard, C. Denage, O. Szajwaj, S. Ito, I. Saadoune, J. Darriet and C. Delmas, *Electrochemical and Solid State Letters*, 2011, **14**, A75.

12 E. Ferg, R. J. Gummow, A. Dekock and M. M. Thackeray, *Journal of the Electrochemical Society*, 1994, **141**, L147; T. Ohzuku, A. Ueda and N. Yamamoto, *Journal of the Electrochemical Society*, 1995, **142**, 1431.

13 M. Shirpour, J. Cabana and M. Doeff, *Energy & Environmental Science*, 2013, **6**, 2538; H. Xiong, M. D. Slater, M. Balasubramanian, C. S. Johnson and T. Rajh, *Journal of Physical Chemistry Letters*, 2011, **2**, 2560; A. Rudola, K. Saravanan, S. Devaraj, H. Gong and P. Balaya, *Chemical Communications*, 2013, **49**, 7451.

14 P. Senguttuvan, G. Rousse, V. Seznec, J.-M. Tarascon and M. Rosa Palacin, *Chemistry of Materials*, 2011, **23**.

15 G. Rousse, M. E. Arroyo-de Domablo, P. Senguttuvan, A. Ponrouch, J. M. Tarascon and M. R. Palacin, *Chemistry of Materials*, 2013, **25**, 4946.

16 S. Lee, Y. Cho, H. K. Song, K. T. Lee and J. Cho, *Angewandte Chemie-International Edition*, 2012, **51**, 8748.

17 J. Xu, D. H. Lee, R. J. Clement, X. Q. Yu, M. Leskes, A. J. Pell, G. Pintacuda, X. Q. Yang, C. P. Grey and Y. S. Meng, *Chemistry of Materials*, 2014, **26**, 1260.

18 M. K. Aydinol, A. F. Kohan, G. Ceder, K. Cho and J. Joannopoulos, *Physical Review B*, 1997, **56**, 1354.

19 W. Ra, M. Nakayama, W. Cho, M. Wakihara and Y. Uchimoto, *Physical Chemistry Chemical Physics*, 2006, **8**, 882.

20 Y. Shiro, F. Sato, T. Suzuki, T. Iizuka, T. Matsushita and H. Oyanagi, *Journal of the American Chemical Society*, 1990, **112**, 2921.

21 M. Venkateswarlu, C. H. Chen, J. S. Do, C. W. Lin, T. C. Chou and B. J. Hwang, *Journal of Power Sources*, 2005, **146**, 204; W. Ra, M. Nakayama, H. Ikuta, Y. Uchimoto and M. Wakihara, *Applied Physics Letters*, 2004, **84**, 4364.